metals

MDPI

Article

Application of Viscous Damper and Laminated Rubber Bearing Pads for Bridges in Seismic Regions

Seyed Saman Khedmatgozar Dolati [1,*], Armin Mehrabi [1] and Seyed Sasan Khedmatgozar Dolati [2,*]

[1] Department of Civil and Environmental Engineering, Florida International University, Miami, FL 33174, USA; AMehrabi@FIU.edu
[2] Department of Civil and Environmental Engineering, University of Texas at San Antonio, San Antonio, TX 78249, USA
* Correspondence: SKhed004@FIU.edu (S.S.K.D.); Seyedsasan.khedmatgozardolati@utsa.edu (S.S.K.D.)

Abstract: Normally, Laminated Rubber Bearing Pads (LRBPs) are directly placed between girders and piers and their role is to provide the bridge span with horizontal movement, and to transmit the gravity loads from the deck to the piers. Although not designed for seismic loads, they can act as a fuse, partially isolating the substructure from the superstructure and keeping the piers intact during earthquakes. However, recent investigations show that large relative displacement of superstructure against substructure caused by sliding at bearing (sliding between girders and LRBPs) can cause expansion joint failure or even bridge span collapse. Accordingly, proper restrainers should be selected to prevent large displacement. Among all types of restrainers, viscous dampers as passive energy dissipation devices have shown a great capacity in damping earthquake energy. This study investigates the effectiveness of a VD-LRBP system, a viscous damper in conjunction with LRBPs, in dissipating energy and reducing the displacement of the superstructure with reference to the substructure caused by sliding at bearing during a seismic event. A Finite Element (FE) model was first developed and validated using available experimental and numerical results. With the validated model, a 3D Nonlinear Time History Analysis (NTHA) was conducted on a reinforced concrete bridge model under various records of earthquakes using OpenSees, an open-source finite element software. The relative displacement histories were recorded for the bridge in two cases: 1- with only LRBPs and 2- with viscous dampers and LRBPs (VD-LRBP system). The results of this study show that applying viscous dampers can reduce the relative displacement of the superstructure with reference to the substructure for up to 60 percent. As importantly, it can also reduce the residual displacement after the earthquake to near zero.

Keywords: base isolation; laminated rubber bearing pads; viscous damper; nonlinear time history analysis; seismic design; earthquake; ground motions; restrainer; opensees; residual displacement

Citation: Khedmatgozar Dolati, S.S.; Mehrabi, A.; Khedmatgozar Dolati, S.S. Application of Viscous Damper and Laminated Rubber Bearing Pads for Bridges in Seismic Regions. *Metals* **2021**, *11*, 1666. https://doi.org/10.3390/met11111666

Academic Editor: Evangelos V. Hristoforou

Received: 23 July 2021
Accepted: 15 October 2021
Published: 20 October 2021

1. Introduction

Highway bridges play a vital role in human life and constitute a substantial portion of national wealth globally as they provide passages over physical obstacles, including valleys, rivers, and intersecting roads. However, during earthquakes, bridges may pose a great danger to public safety. In recent earthquakes, namely, the 1994 Northridge earthquake, the 1999 Chi-Chi earthquake, the 2008 Wenchuan earthquake, and the 2010 Chile earthquake, many highway bridges collapsed or partially failed [1–5]. Failures caused by earthquakes can incur a lot of direct and indirect costs as essential routes might be cut off, delaying the post-earthquake rescue operation. Typical damages for highway bridges include damages to substructure, superstructure, and foundation elements in general that may result in the collapse of bridge spans in longitudinal and transverse directions. Sliding and unseating of superstructure can also occur during the earthquake. Much research has been conducted for designing the bridge elements, including connections and structural elements as well as restrainers against sliding and unseating, to prevent catastrophic

failures. Most noticeable and drastic collapses have been associated to transverse direction. This study concentrates on lateral behavior of simply supported bridges under seismic loading in transverse direction. However, the results are also applicable to longitudinal direction with relevant considerations.

The application of Laminated-Rubber Bearing Pad (LRBP) is a common method for seating of deck elements on piers and supports for simply supported multi-span bridges. They are also expected to allow thermal movement of the superstructure at the service-level condition but, in most cases, they have not been designed for seismic loads. They are placed directly between girders and pier caps and allow sliding of superstructure [6–8]. In 2020, Barmi and Khaloo investigated the lifetime performance of unbonded rubber bearing in bridges. In their wok, 13 full-scale steel-reinforced elastomeric bearing specimens were constructed and tested to explore the effect of the long-term presence of vertical loads on the mechanical properties of the bearings. The results of their research indicated that although the long-term vertical loading can slightly change the vertical and shear stiffness and damping coefficient of bearings, their lifetime performance is satisfactory, and they can act as an isolation system [9]. In 2021, Xiang et al. studied the effect of bearing installation method on the overall seismic behavior of bridges. In their work, after observing the typical bearing damages in the past major earthquakes in Japan and China, a new improved design option was suggested in which top-side bonded elastomeric was used [10]. Zhang et al. (2021) investigated the seismic performance of the laminated rubber bearing in bridges based on an Artificial Neural Network (ANN). In their work, a new constitutive model of bearing based on the ANN technique was established through the static cyclic test of laminated rubber bearings, considering the bearing mechanical properties. After performing various tests and analyses, they concluded that the main factors affecting the bearings constitutive model are vertical load and dimensions of the bearing. In addition, they found that the height of bearing is the most critical factor affecting the seismic response of bridges [11]. Damage investigation on small- to medium-span highway bridges with LRBPs has indicated that their typical damages include: (a) the failure of the shear key, (b) joints and abutment failure, and (c) span collapse [12,13]. Lessons learned from the Chi-Chi earthquake in 1999 and the Wenchuan earthquake in 2008 showed that there have been minor or no cracks in piers for bridges experiencing sliding at bearing (sliding between LRBPs and girders).

It can be justified that sliding at bearing can act as a fuse that isolates the substructure from the superstructure reducing the inertia forces transmitted from deck to the piers [14–16]. Filipov et al. (2013) [17,18] and Steelman et al. (2013) [19] experimentally and numerically investigated the sliding effect of rubber bearing in Illinois bridges. They found that rubber bearing limited the seismic force transmitted to the substructure members while providing for the associated displacement. However, the large displacement of the superstructure against the substructure caused by sliding at bearing can be an issue. Indeed, excessive sliding can cause expansion joint failure or even span collapse during extreme earthquakes [14,15]. Therefore, appropriate restrainers should be selected and designed to reduce the displacement associated with sliding at bearing and to dissipate the earthquake energy.

Among all types of passive restrainers, energy dissipation devices have shown promise for limiting seismic damage. Viscous dampers and yielding metallic dampers are the most common types of energy dissipation restrainers. Viscous dampers have been widely used to reduce the dynamic response of bridges [20,21]. Liu et al. (2021) investigated the effect of viscous dampers in dynamic response of a pedestrian bridge subjected to a set of ground motions. After performing several analyses, they concluded that installation of linear viscous dampers can effectively improve the seismic performance of bridges if the optimized damping coefficient and velocity are used [22]. In 2020, Hu et al. proposed a design method for a damped structure based on the specified damping distribution pattern. After validation of the proposed method and conducting various analyses, they concluded that concept of damping distribution can significantly improve the seismic mitigation

efficiency [23]. Yielding metallic dampers, also referred to as added damping and stiffness (ADAS), dissipate the seismic energy through the inelastic behavior of metallic substances. Using ADAS dampers also provides bridges with supplement stiffness that control the relative displacement of sup- against sub-structure [24,25]. In 2021, Nguyen and Guizani analytically and numerically investigated the cyclic behavior of natural rubber bearings (NRB) incorporating U-shaped dampers (UD). In their work, a set of UDs and NRBs were subjected to cyclic loadings, and the effect of different parameters including geometric and loading on their performance were investigated. The results of their work indicated that NRB-UDs systems can be practiced for bridges as an isolation system with high energy dissipation capacity with stable hysteresis behaviors in any direction [26]. In 2016, Li et al. investigated the implementation of X-steel damper (XADAS) and laminated rubber bearing pads as an innovative method to prevent span collapse by dissipating seismic forces and controlling relative displacement for RC highway bridges. In their work, a quarter-scale two-span RC bridge model was constructed and tested on a shake table. Northridge and artificial ground motions in transverse direction were applied to the model to evaluate its seismic performance. Both numerical and experimental results showed the effectiveness of implementing X-steel dampers in conjunction with laminated rubber bearing pads for controlling the relative displacement between girders and piers, and for protecting piers from severe damage during earthquakes [7].

The application of passive restrainers in conjunction with LRBPs is a new approach for controlling the large movement of the span. This combination has recently been investigated for reducing damages from earthquake in longitudinal direction for continuous bridge spans [27,28]. In the transverse direction, while the use of XADAS dampers in conjunction with LRBPs has been studied [29], little or no research has been conducted on the application of viscous dampers for the bridges combined with LRBPs. Viscous dampers (VD) can be a proper replacement for other types of restrainers because of their easy maintenance and since they can be easily retrofitted after the earthquake. To be able to provide bridges with an effective isolation system under various earthquakes, it is essential to evaluate the behavior of restrainers (XADAS and viscous dampers, etc.) in conjunction with LRBPs in reducing the large relative displacement. Additionally, the application of restrainers by adding stiffness to the system has the potential to increase the inertia forces transmitted to the piers and therefore needs to be investigated. Accordingly, the force produced into the piers should be monitored. It goes without saying that nonlinear analysis provides for more realistic and accurate evaluation methods, and as such, this method of analysis is selected for analysis of the bridge under dynamic loads. If proper passive energy devices cannot be identified for an application, at best, it can be a waste of money, and at worst, it can cause irreparable damage to the bridge under earthquake loads.

This study aims at investigating the effectiveness of a VD-LRBP system, viscous dampers for bridges in conjunction with LRBPs, in limiting the relative displacement of super-structure against sub-structure under various earthquakes in transverse direction. 3D Nonlinear Time History Analysis (NTHA) of a reinforced concrete bridge has been conducted to evaluate the effectiveness of the proposed system. OpenSees, an open-source finite element analysis software, has been used for modeling of the bridge. The results of this study show the effectiveness of the application of viscous damper in reducing the large displacement caused by sliding at bearing and for dissipating the earthquake energy. As importantly, applying viscous dampers shows reduction in residual displacement that might exist after the earthquakes. The introduced system is economical; labor-friendly; and can be added, repaired, or changed easily after an earthquake. It is expected that this study will help the proliferation of the application of the proposed system in seismic areas.

The major contribution of this study is investigating and proving the effectiveness of the combined LRBPs and viscous dampers in reducing or eliminating sliding of the superstructure with respect to supports. To accomplish this, 3D nonlinear time history analysis (3D NTHA) validated with the experimental results was used for accurately simulating the seismic behavior against several reference ground motions.

2. Application of VD-LRBP System for Highway Bridges

Based on the American Association of State Highway and Transportation Officials, AASHTO LRFD Bridge Design Specifications [30], when using fusing devices, both the super- and sub-structure of a bridge shall remain elastic during an earthquake. The system considered in this study includes both LRBP and viscous damper working simultaneously during an earthquake. The LRBPs are placed between the girders and piers (Figure 1). Their role is to transfer all load on the bridge deck to the pier, reduce the pier vibration, and provide for the horizontal movement of the bridge spans. LRBPs usually are not designed for seismic loads. However, the sliding between LRBPs and girders (sliding at bearing) under earthquakes can potentially and partially isolate the superstructure from the substructure. Accordingly, sliding at bearing can limit the inertia force transmitted from the superstructure to the piers.

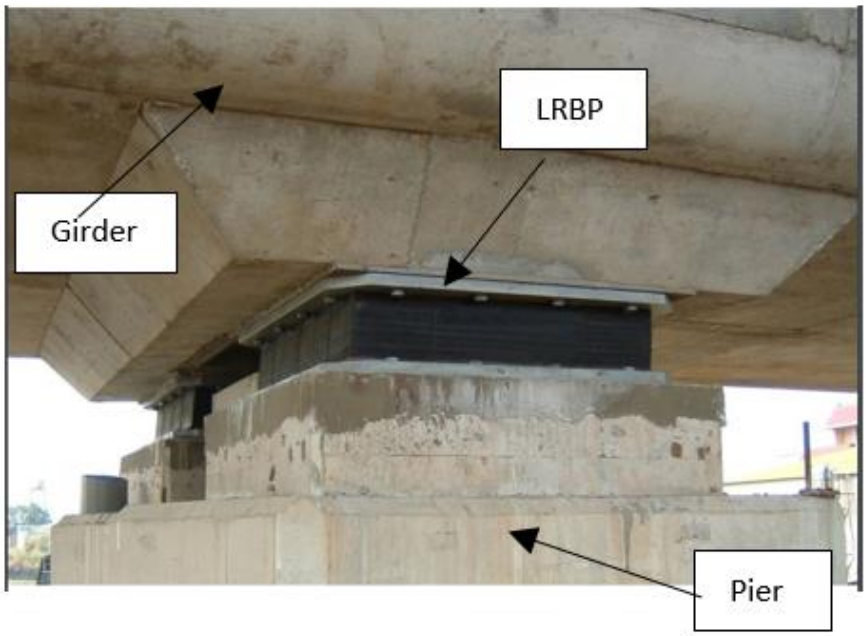

Figure 1. Laminated rubber bearing Pad (LRBP) reproduced from [31].

In the VD-LRBP system, viscous dampers are placed in conjunction with LRBPs in the direction of the earthquakes (Figure 2). Their role is to dissipate earthquake energy and control the large relative displacement between girders and piers caused by sliding at bearing, and to prevent expansion joint failure or span collapse.

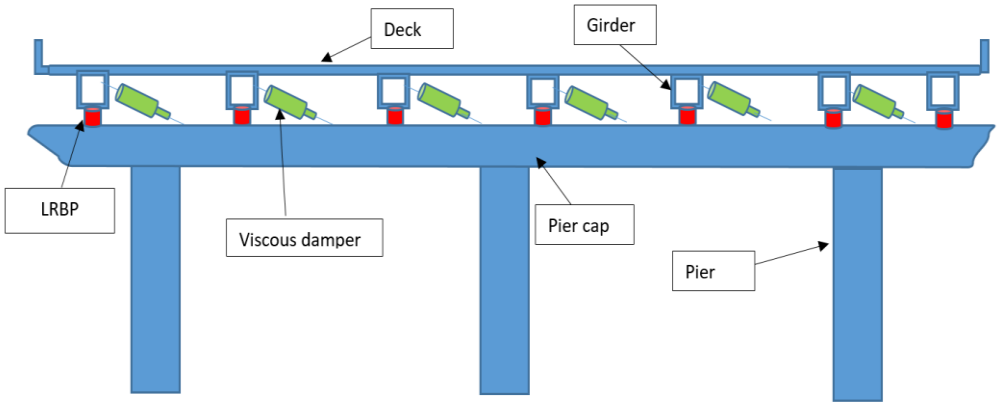

Figure 2. Schematic of the proposed system.

In applying this system following points should be taken into account:

- LRBPs are placed between the girders and piers with no restraint of horizontal motion other than friction. Therefore, they only carry out the gravity load and transmit it to the substructures. On the other hand, dampers are not participating in transferring the gravity loads. They dissipate earthquake energy and provide the bridge with lateral stiffness. Accordingly, the increased lateral stiffness of the bridge reduces the relative displacement between piers and girders;
- In the proposed configuration, the dampers are connecting the side of the girder to the top of the pier cap. As such, dampers and LRBPs perform as a parallel system, and their displacements are equal. The system acts in series with the piers. This distinction is required for accurate modeling in finite element analysis.

Viscous Damper

Dampers are usually used to mitigate the seismic response of structures. They have shown great energy-dissipation capacity under dynamic loads. Typically, dampers dissipate energy through yielding, material failure, or loss of energy due to flow of viscous liquid through orifices. One type of damper that has shown great performance under dynamic loads is viscous dampers (Figure 3) [32]. This type of damper controls motion by providing a force or torque opposing the motion proportional to the velocity. Viscous dampers have been widely implemented in bridges for seismic regions. There has been much research in terms of the implementation of the viscous damper in long-span bridges, including cable-stayed [33–37] and suspension bridges [38,39]. A well-known practical application of this type of damper can be found in the cable-stayed Greek Rion-Antirion bridge located in a highly active seismic area.

Figure 3. Viscous damper reproduced from [40].

The use of proper viscous dampers protects the structural components during an earthquake. The damper force which resists the structure motion is calculated according to the damping law (Equation (1)):

$$F = CV^{\alpha}. \quad (1)$$

where F is the damper force, C is a constant number that remains constant over the full (effective) range of velocities and displacements, V is velocity, and α is an exponent that can range from 0.3 to 1.95. As can be seen in equation one, there is no spring force, so the damping force is dependent on the velocity of the two ends of the damper. Figure 4 shows the components of a typical viscous damper.

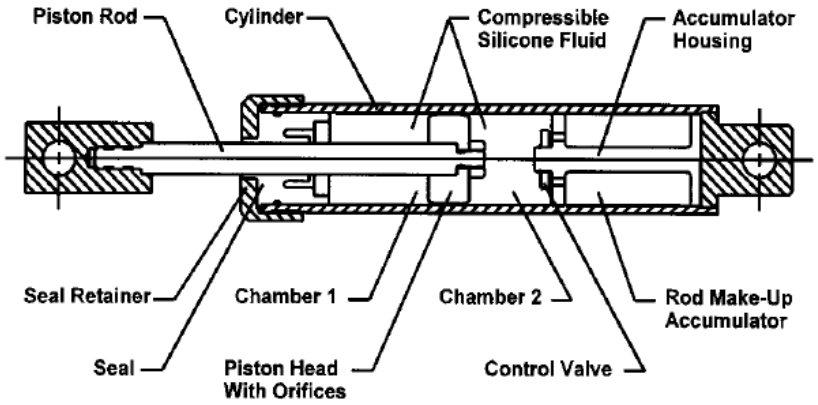

Figure 4. Typical components of viscous damper reproduced from [41].

In viscous dampers, when the piston moves, the fluid is pushed through the piston heads and around the orifices. The velocity of the fluid in this region is high. Therefore, the upstream pressure energy converts to kinetic energy. The fluid slows down and loses its kinetic energy to turbulence when moving through orifices and on the other side of the piston head. On the downstream side of the piston head, there is very little pressure compared to the upstream side of the piston head that experiences the total pressure. The difference in pressures causes a large force that resists damper motion.

The material of viscous damper elements should be chosen carefully; otherwise, the service life of the dampers will be shorter than expected (less than 35 years) [42]. According to the OSHA (Occupational Safety & Health Administration) guidelines, a flashpoint of fluid should be at least 200 degrees of Fahrenheit. Currently, silicon fluid with a flashpoint of 650 degrees of Fahrenheit is used in most viscous dampers. This fluid is cosmetically inert, nontoxic, and thermally stable. The cylinder should be made up of seamless steel tubing and must be able to withstand 1.5 times the damper operational pressure loading. The piston rod should be selected from high alloy stainless steel. It is designed for rigidity to be able to resist compression buckling and flexure under dynamic load.

As shown in Equation (1), the damper force is exponentially varying with α, the power of the damper. Figure 5 shows the force-velocity plot for several values of α. When α is equal to one, the curve shows linear damping. The hysteresis loop for a linear damper is a pure ellipse. The lowest damping exponent normally possible is 0.3. As the power (α). decreases, more force at a lower velocity will be produced. Figure 6 shows the hysteresis loops (force-deflection plot) for a viscous damper with α. equal to 1 and 0.3. Any value above one is not accepted since it produces very poor performance [42].

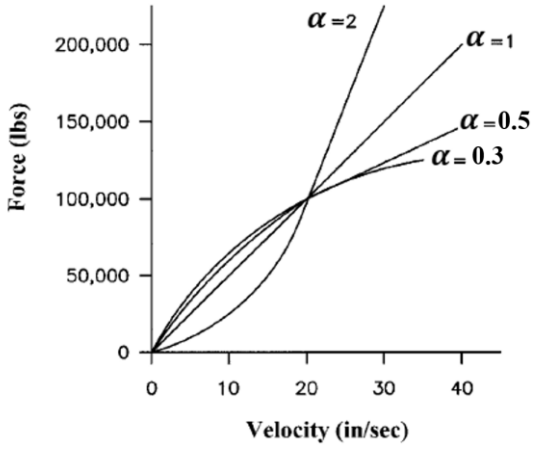

Figure 5. Plot of force against velocity for several values of the damping exponent modified from [42].

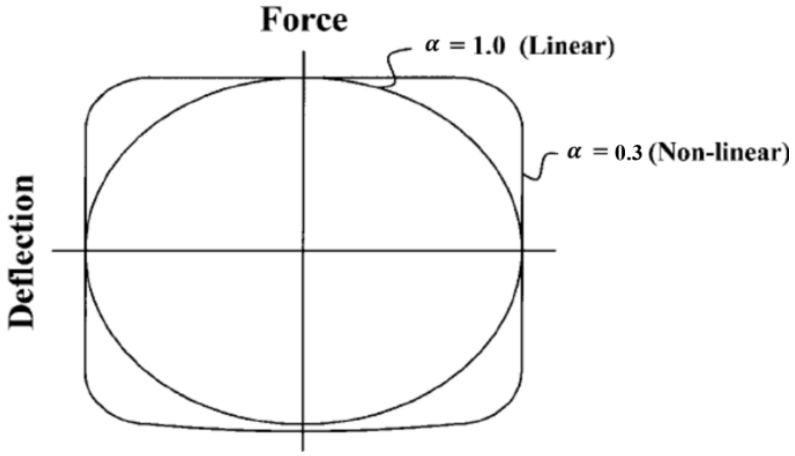

Figure 6. Hysteresis loops for linear and nonlinear dampers for two values of the damping exponent modified from [42].

3. Finite Element Analysis

The objective of this study is to demonstrate that the VD-LRBP system offers great advantages over using only LRBP. To address this, a series of finite element analyses is performed on bridge models that include these systems. Before attempting such analysis, the modeling technique needs to be verified with valid experimental results. For this verification, a simple span model with LRBPs tested by Xiang et al. (2018) is chosen, for which experimental results are available. However, for the VD-LRBP system performance, a more elaborate bridge model with a range of modal shapes and frequencies is desirable. Therefore, for the main analysis demonstrating the behavior of VD-LRBP system, a two-span bridge model was used.

3.1. Validation of the Finite Element Model

3.1.1. Bridge Model

The bridge model used for validation is a case study of a RC highway bridge in Wenchuan, China. Xiang et al. (2018) fabricated a single span quarter-scale model of that bridge in the laboratory and investigated the effectiveness of the X-steel (XADAS) damper and concrete shear key in conjunction with LRBPs in reducing the relative displacement between superstructure and substructure caused by sliding at bearing. Figure 7 shows this laboratory bridge model and its details.

For comparison and verification of the model developed in this study, seismic analysis of the bridge model was conducted using OpenSees, an open-source finite element analysis software. This analysis compared the behavior only with LRBPs in place. Figure 8 shows the 3D finite element model of the bridge also showing the location of LRBPs. This finite element model is similar to the model used by Xiang et al. (2018) [43]. The modeling details are described in the following sections.

3.1.2. Beam

For modeling beams in OpenSees, elastic beam-column elements are used. To be able to define this element, the cross-sectional area of the beam element, Young's modulus, shear modulus, the torsional moment of inertia of cross-section, second moment of area about the local z-axis and y-axis, and coordinate-transformation (CrdTransf) object are needed. Table 1 shows these calculated values.

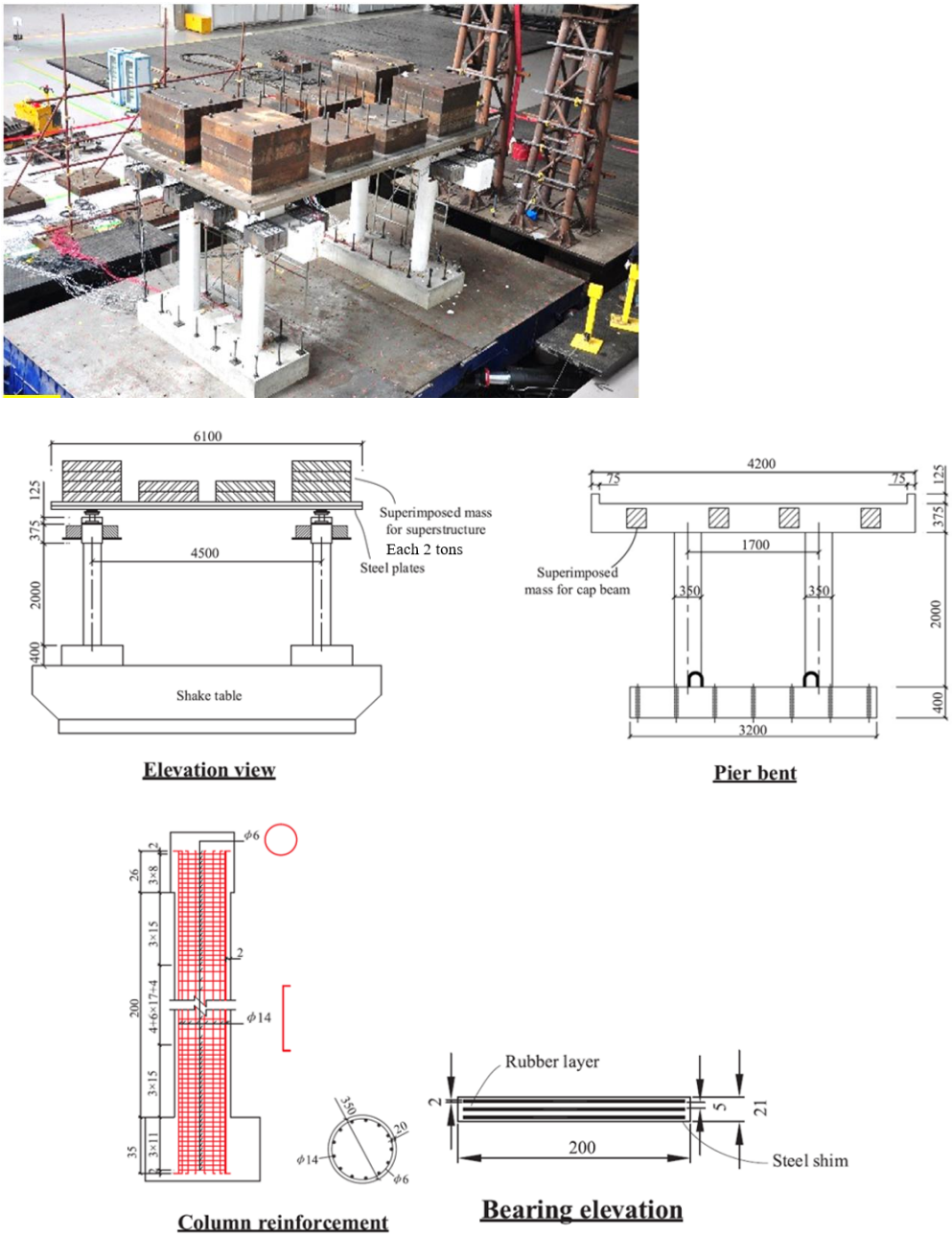

Figure 7. Details of the bridge model [unit: mm]. Reprinted with permission from ref. [43]. Copyright Elsevier.

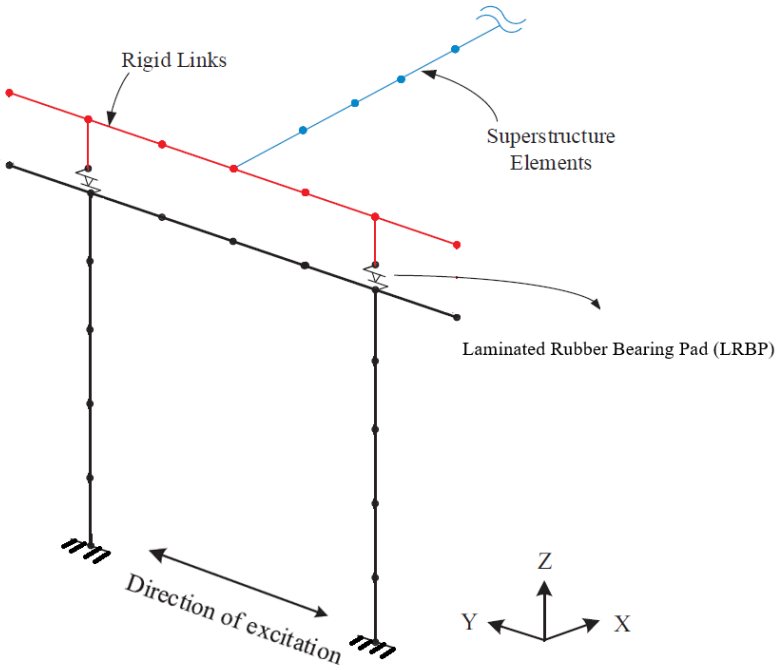

Figure 8. Finite element modeling of the bridge with the location of LRBPs.

Table 1. Modeling the beams in the OpenSees.

Beam Elements		
Command:	**Element elasticBeamColumn**	**SI Units (m, k, s)**
A	cross-sectional area of element	1.54
E	Young's Modulus	3.27×10^{10}
G	Shear Modulus	1.25×10^{10}
J	Torsional moment of inertia of cross section *	1.8×10^{-2}
Iz	Second moment of area about the local z-axis *	1.8×10^{-2}
Iy	Second moment of area about the local y-axis *	1.8×10^{-2}
transfTag	Identifier for previously-defined coordinate-transformation (CrdTransf) object	(0, 0, 1)

*: These factors have negligible influences on the overall seismic response of the scaled model.

3.1.3. Columns

For modeling columns, the displacement-based beam-column element is used (considering 5 integration points along the element). This element considers the spread of plasticity along the column. Using this element depends on the previously defined section. The fiber section command is used for the needed section. This section is composed of fibers, with each fiber containing a uniaxial material, defining the cross-section of the columns. To be able to consider the role of shear reinforcement in the column, two types of material for concrete, confined concrete and unconfined concrete, are considered (Figure 9). Tables 2–4 show the material properties for confined and unconfined concrete as well as reinforced bars, respectively.

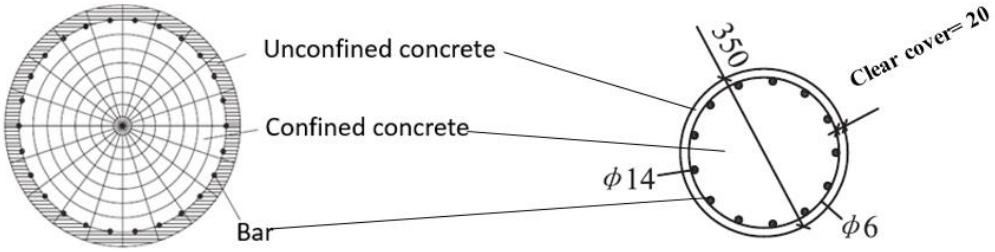

Figure 9. Fiber section defining the column cross-section.

Table 2. Confined concrete material properties.

Material Properties of Confined Concrete (Units: Pascal (N/m^2))		
Command	**uniaxialMaterial Concrete01**	
fpc	concrete compressive strength at 28 days (compression is negative)	4.8×10^7
epsc0	concrete strain at maximum strength	4×10^{-3}
fpcu	concrete crushing strength	3.36×10^7
epsU	concrete strain at crushing strength	2×10^{-2}

Table 3. Unconfined concrete material properties.

Material Properties of Unconfined Concrete (Units: Pascal (N/m^2))		
Command	**uniaxialMaterial Concrete01**	
fpc	concrete compressive strength at 28 days (compression is negative)	4×10^7
epsc0	concrete strain at maximum strength	3×10^{-3}
fpcu	concrete crushing strength	2.8×10^7
epsU	concrete strain at crushing strength	1.5×10^{-2}

Table 4. Steel bars material properties.

Material Properties of Reinforcing Bars (Units: N and Pascal (N/m^2))		
Command	**uniaxialMaterial Steel02**	
Fy	yield strength	4×10^8
E	initial elastic tangent	2×10^{11}
b	strain-hardening ratio (ratio between post-yield tangent and initial elastic tangent)	4×10^{-3}

3.1.4. Laminated Rubber Bearing Pad (LRBP)

For simulating the sliding at LRBPs, the Flat Slider Bearing Element from the OpenSees library is used (Figure 10). The flat slider bearing element constructed and calibrated by Li et al. (2016) was used to model 250 × 350 × 63 mm LRBPs. According to their experimental result, the kinetic friction showed independent of sliding velocity and therefore, a Coulomb Friction model was used to define the friction/sliding behavior. The friction coefficient and the initial stiffness of 0.36 and 1400 kN/m were adopted, respectively, from the results obtained by Li et al. (2016). Table 5 shows the details for modeling the behavior of LRBP.

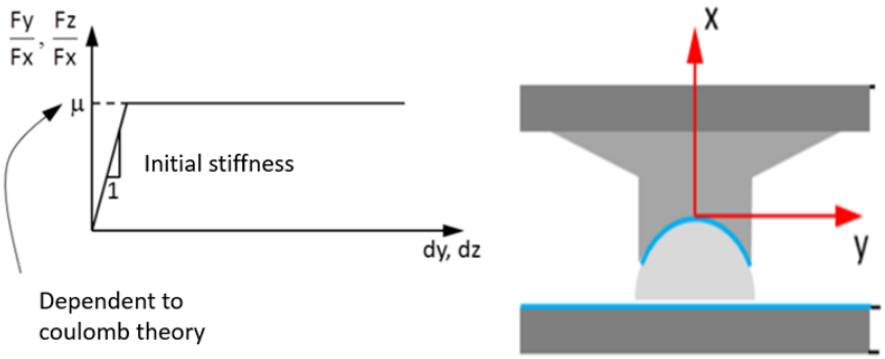

Figure 10. Flat slider bearing element.

Table 5. Details of the modeling of the LRBP.

Modeling the LRBP (Units: Pascal (N/m^2))		
Command	**Flat Slider Bearing Element**	
frnMdlTag	previously-defined FrictionModel	Coulomb Friction
kInit	initial elastic stiffness in local shear direction	1.4×10^6
P matTag	previously-defined UniaxialMaterial in axial direction	Rigid
T matTag	previously-defined UniaxialMaterial in torsional direction	
My matTag	previously-defined UniaxialMaterial in moment direction around local y-axis	
Mz matTag	previously-defined UniaxialMaterial in moment direction around local z-axis	

3.1.5. Viscous Damper

The viscous damper has a velocity-dependent mechanism, and its behavior relies on two factors, the damping coefficient and power factor. For modeling the viscous damper behavior, Two Node Link Element (Figure 11) is used in which Uniaxial Viscous Material is given to the element in the direction of excitation. This material is defined by two parameters, C and α. Dampers of different properties will affect differently the seismic behavior of the model. In this paper, an example damper was adopted from [44,45] which already has optimized with the C and α value of 2×10^4 and 0.5 respectively.

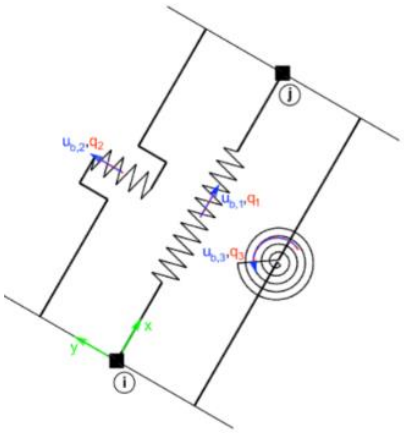

Figure 11. Two Node Link Element in OpenSees.

3.1.6. Verification of Finite Element Model

To demonstrate that the finite element model developed in this study is capable of predicting bridge seismic behavior, analysis is conducted using the model to simulate the

laboratory experiment performed by Xiang et al. [43] as explained above with only LRBPs (no damper). Xiang et al. used Northridge ground motion, shown in Figure 12, for the laboratory experimentation. Therefore, finite element analysis was also performed under the same record for comparison. Figure 13 compares the numerical and experimental results for the displacement histories of the superstructure with reference to the substructure (bearings displacement) at PGA (Peak Ground Acceleration) = 0.2 g.

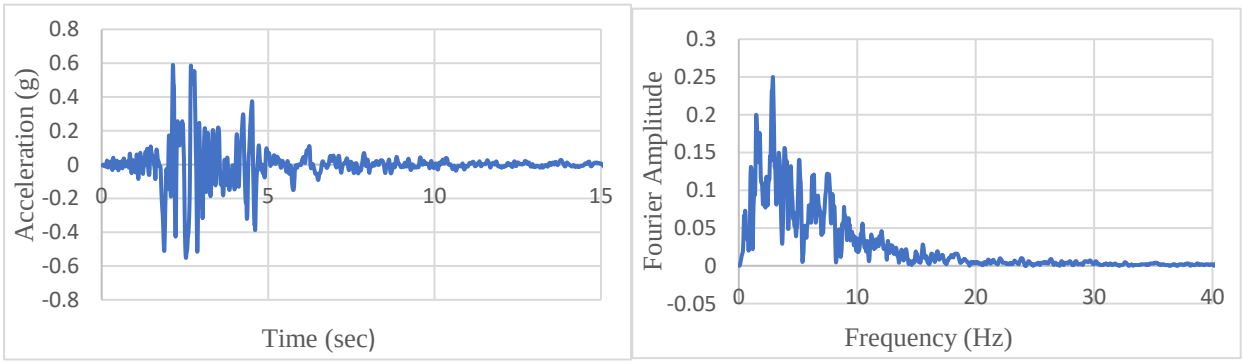

Figure 12. Ground motion record and Fourier spectra: Northridge earthquake.

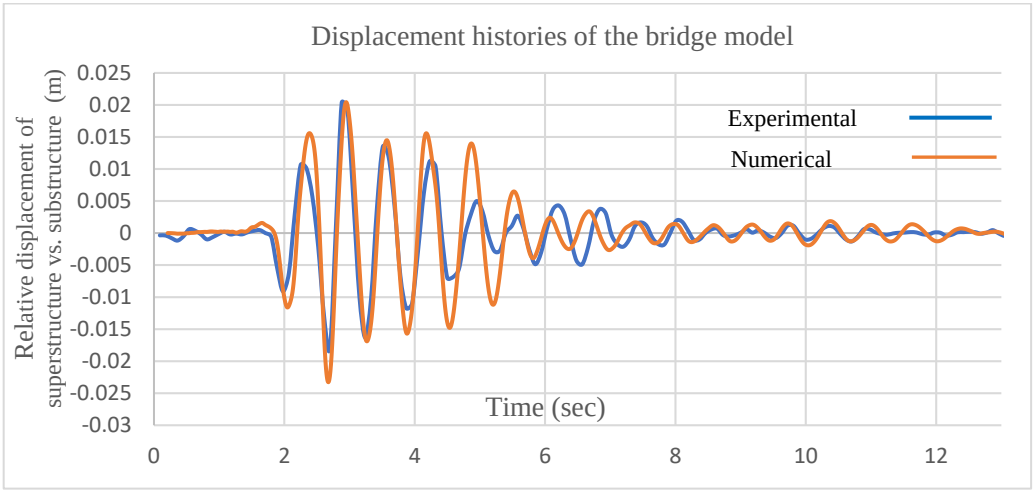

Figure 13. Displacement histories of the superstructures against substructure (bearings displacement) under Northridge earthquake with PGA = 0.2 g.

As shown in Figure 13, there is a good correlation between the experimental and numerical results, especially as it concerns the maximum/minimum displacements and vibration frequency. Therefore, the model is deemed capable of predicting the response of the bridge installed with the LRBP system with good accuracy. For the modeling purpose, the viscous dampers (VD) are modeled using generally accepted constitutive relations proven to accurately simulate the behavior of these devices.

3.2. Analysis for VD-LRBP System Performance

The bridge that is analyzed in this study for evaluating the effectiveness of the proposed system is a two-span bridge with the same properties as that used by Xiang et al. (2018). Accordingly, the finite elements and parameters described above are used for modeling in this analysis. The model now includes both LRBP and viscous damper for corresponding cases. Figure 14 shows the 3D finite element model of the bridge also showing the location of viscous dampers and LRBPs. This model of the bridge is similar to a $\frac{1}{4}$-scale model used by Li et al. (2016) [7].

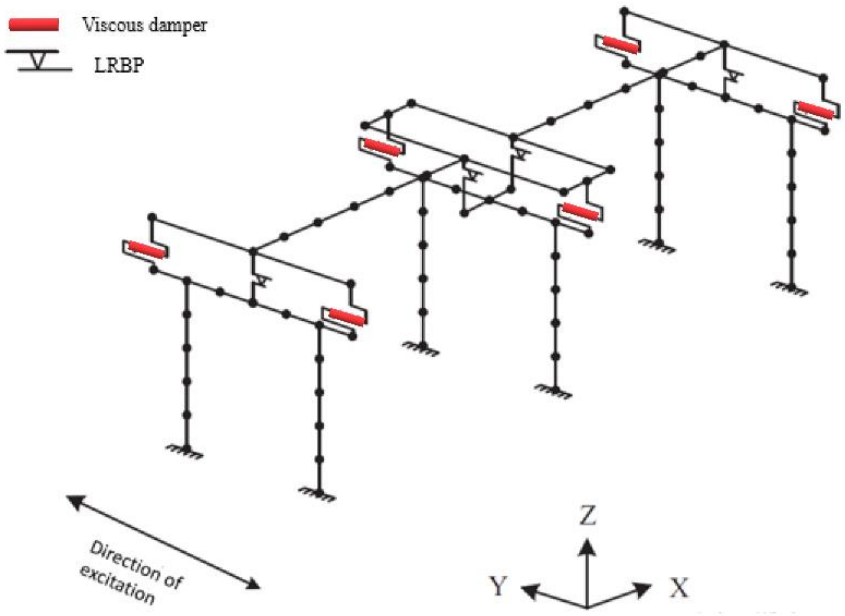

Figure 14. Finite element modeling of the bridge with the location of viscous dampers and LRBPs.

To demonstrate the effectiveness of the new system, the finite element model of the bridge is used to simulate the behavior for various ground motions records.

Selected Ground Motions

The Nonlinear Time History Analysis (NTHA) of the model, an accurate method in predicting the response of the bridge, is conducted under four different seismic records. The Northridge earthquake in 1994 recorded in Newhall Fire station (Figure 12) was used for initial investigation and fine tuning of the viscous damper for optimal performance. Subsequently, three other ground motion records, the TABAS (Iran) earthquake in 1978 (Figure 15), the Kobe (Japan) earthquake in 1995 recorded in Takarazuka station (Figure 16), and Imperial Valley in 1979 recorded in El Centro station (Figure 17), were used in this study to show reproducibility of the results. The latter is important to demonstrate that the positive effects of the new system can be repeated for the case of other ground motions. In the meantime, the approach used in this study can be utilized for further refinement to produce the best possible results for any specific ground motion and bridge structure. The ground motion data were extracted from the PEER ground motion database website (https://ngawest2.berkeley.edu/, accessed on 15 January 2021). The time axis of the ground motions was scaled to 0.5 (according to similitude rules, this is the square root of the 1/4 scale of the model). Table 6 shows the details of the selected ground motions.

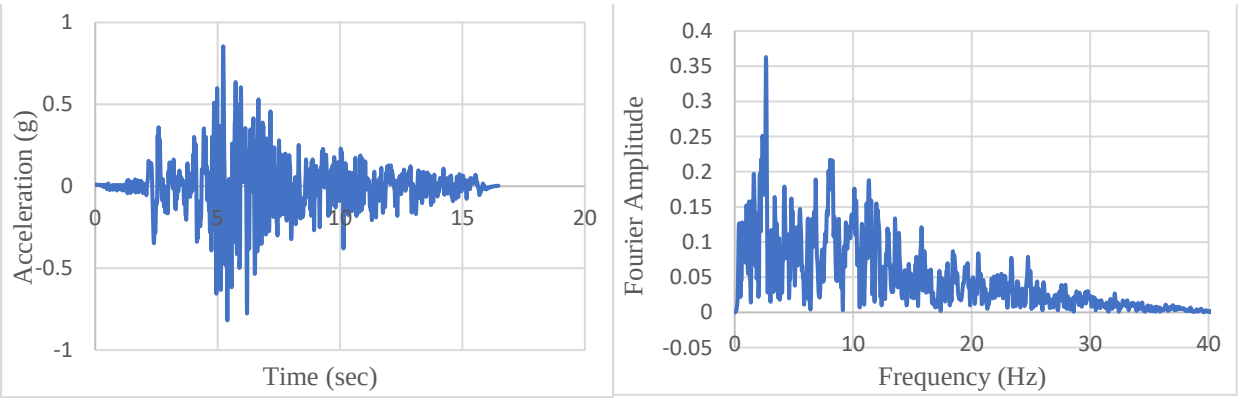

Figure 15. Selected ground motion record and Fourier spectra: Tabas earthquake.

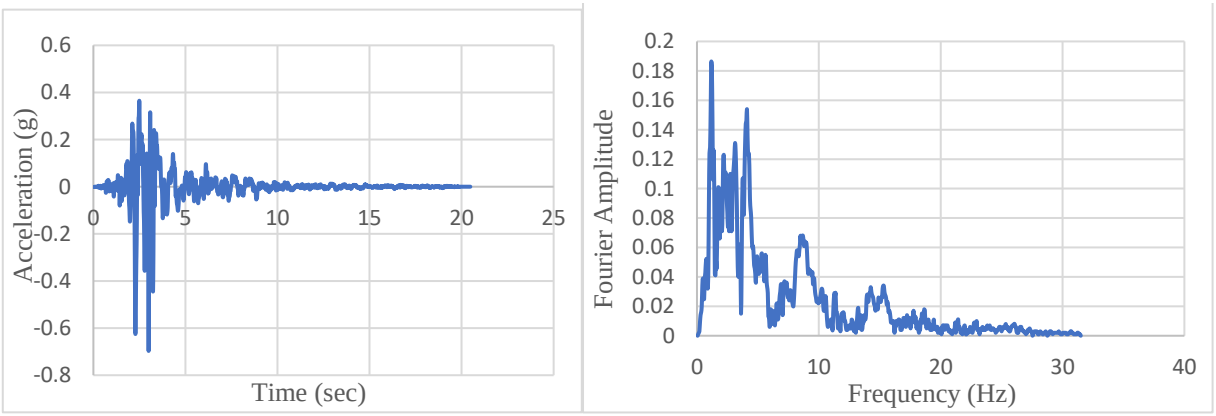

Figure 16. Selected ground motion record and Fourier spectra: Kobe (Japan) earthquake.

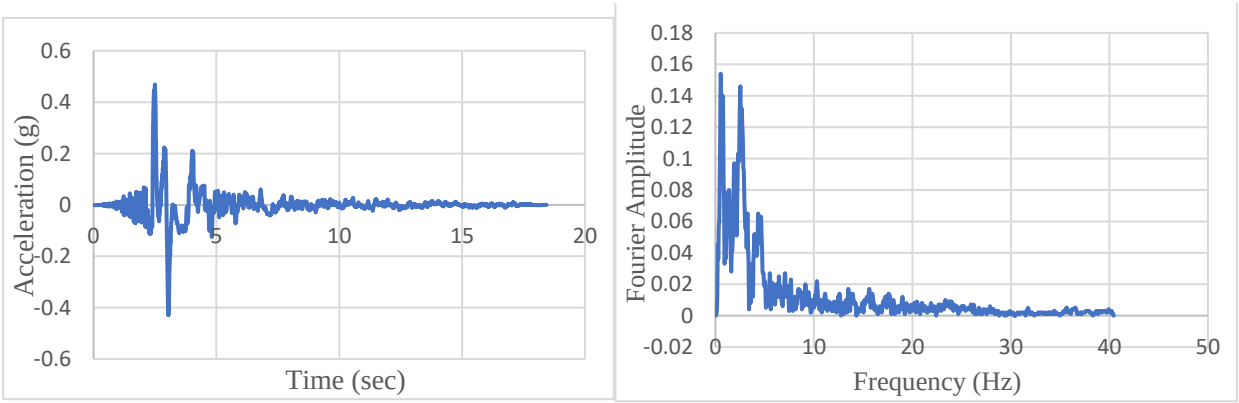

Figure 17. Selected ground motion record and Fourier spectra: Imperial Valley (El Centro) earthquake.

Table 6. Selected ground motions.

Earthquake Station	RSN (s)	Magnitude
Northridge Newhall Fire	1044	6.69
TABAS	143	7.35
Kobe (Japan)	1119	6.9
Imperial Valley (El Centro)	182	6.53

4. Performance of VD-LRBP under Northridge Ground Motion

To demonstrate the effectiveness of the VD-LRBPs system in reducing the relative displacement of the superstructure with reference to the substructure (bearings displacement) under Northridge ground motion, 3D Nonlinear time history analysis was conducted on the bridge model in two cases, one with LRBPs only and the other with LRBPs combined with viscous damper. The ground motion was applied with an intensity of 0.4 g in the transverse direction.

Figure 18 shows the relative displacement of the superstructure with respect to the substructure (bearings displacement) under the 3D nonlinear time history analysis. It indicates the responses with only LRBPs (blue curve) and with LRBPs combined with the viscous dampers (orange curve), under the Northridge earthquake. It can be seen that the maximum relative displacement for the case of only LRBPs is 73 mm. However, with the proposed system (VD-LRBP), it is reduced to 30 mm.

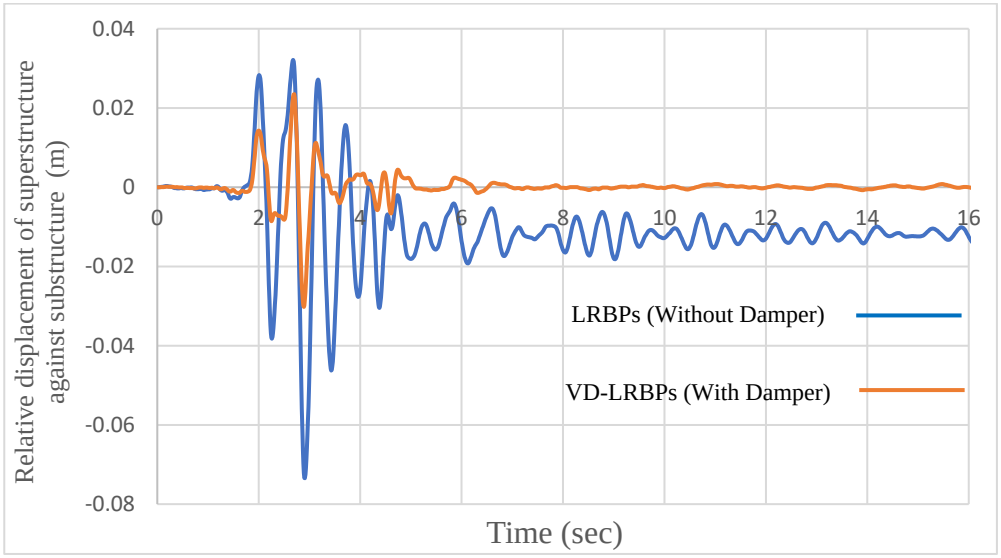

Figure 18. The relative displacement of superstructure versus substructure histories under Northridge earthquake.

As importantly, in the case of only LRBPs, the bridge model experienced residual displacement after the earthquake. This residual displacement is due to the large sliding at the bearings. However, the proposed system prevents excessive displacement at the bearings and reduces the potential residual displacement to near zero.

The force that Pier 1 (see Figure 14) experienced during the earthquake was also recorded (Figure 19). In the case of only LRBPs, the maximum force is 13,113 N, and for the case of VD-LRBPs, this force is 15,732 N. This increase can be justified by the fact that the viscous damper has the potential to add stiffness to the bridge model, which increases the inertia force transmitted from superstructures into the piers. However, although required to account for the design of the substructure, due to the highly beneficial contribution of the viscous damper in dissipating the earthquake energy, this increase is relatively small and should not cause major concern.

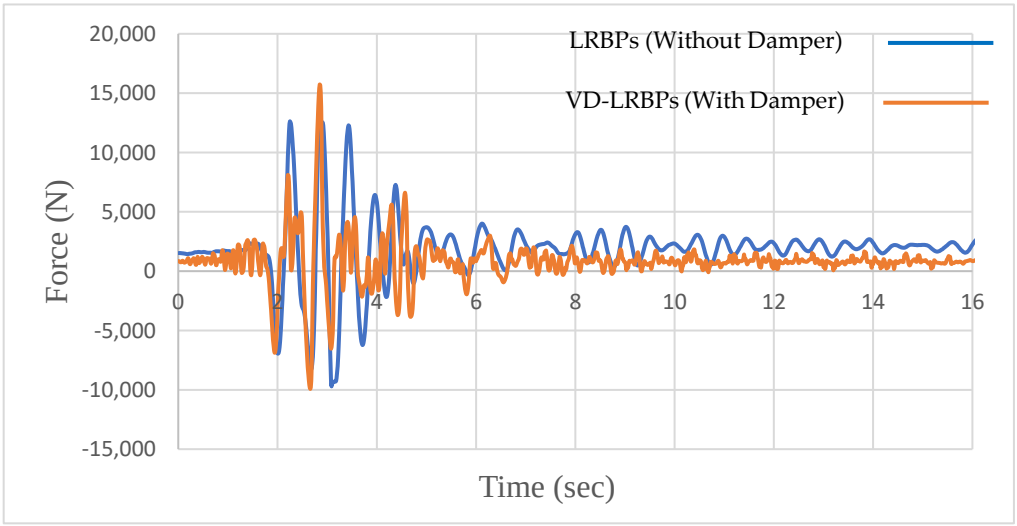

Figure 19. Force histories that pier 1 experiences under the Northridge earthquake.

5. Reproducibility and Repeatability of the System Effectiveness

To investigate the reproducibility of the results and repeatability of the effectiveness of the proposed system, the bridge model was also analyzed for three other ground

motion records with and without viscous dampers. The results are described in the following sections:

5.1. Tabas Ground Motion Record

Figure 20 shows the relative histories of the displacement of superstructure with respect to the substructure under the Tabas earthquake. It can be seen that the maximum relative displacement for the case of only LRBPs is 39 mm, where, by implementing the VD-LRBPs system, it is reduced to 18 mm.

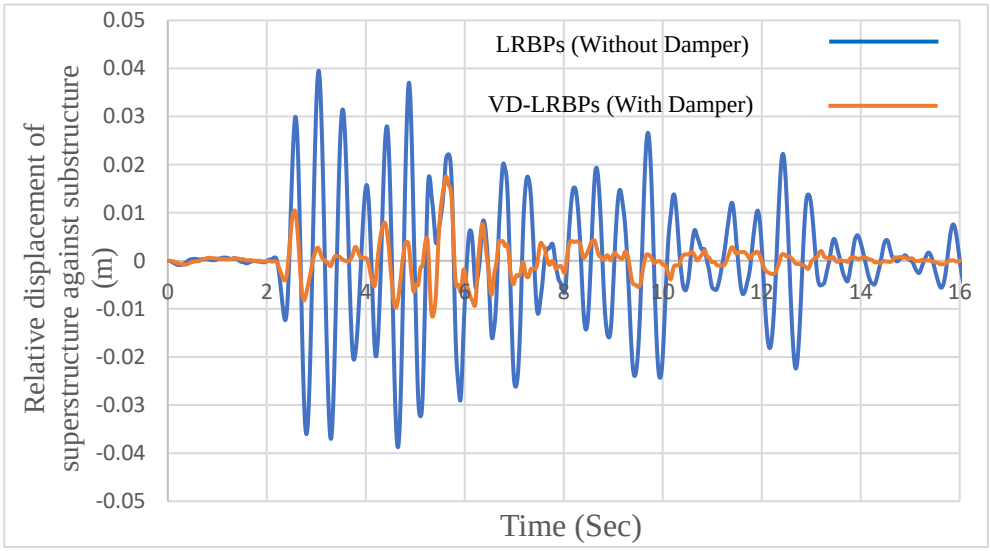

Figure 20. The relative displacement of superstructure versus substructure histories under Tabas earthquake.

The maximum force that pier one experienced under the Tabas earthquake is 12,620 N for the case of only LRBPs. However, this amount is reduced to 9216 N in the case of implementing the new system (Figure 21). As it can be noticed, the combination of LRBP and VD shows significant benefits for both displacement and force. This can be attributed to fitness of the design of the VD to the inherent behavior of the bridge under this specific ground motion record.

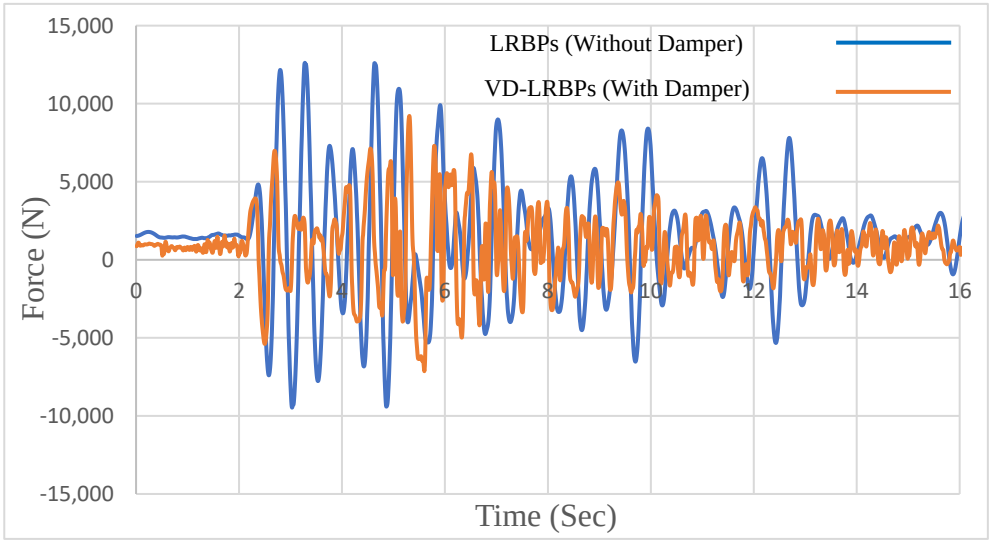

Figure 21. Force histories that pier 1 experiences under the Tabas earthquake.

5.2. Kobe Ground Motion Record

The maximum bearings displacement for the case of only LRBPs is 47 mm, while, for the case of the VD-LRBPs system, it is reduced to 17 mm (Figure 22). Furthermore, Figure 22 shows that the bridge model experiences residual displacement in the case of implementing only LRBPs. However, the residual displacement is reduced to near zero with the application of the proposed system.

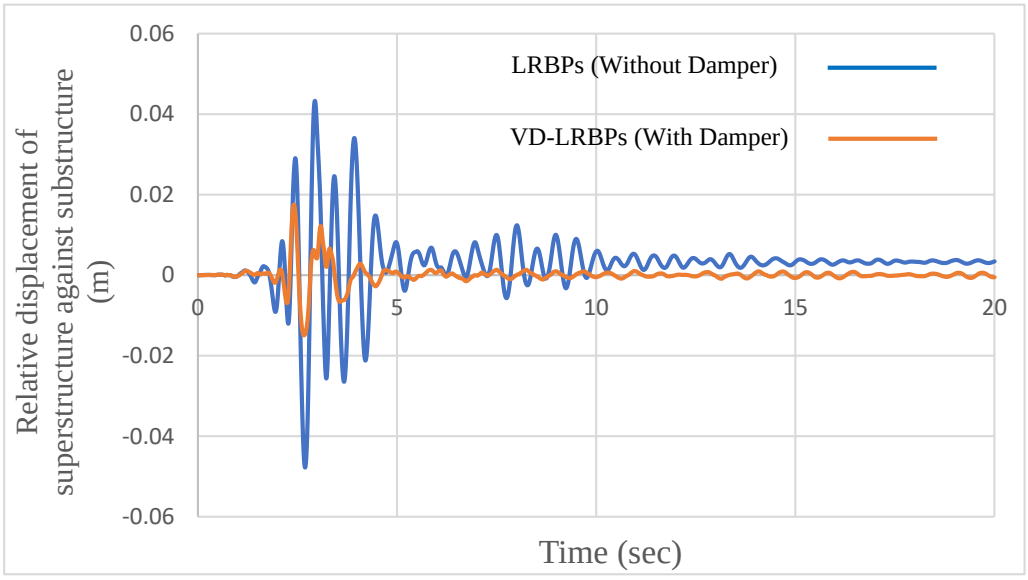

Figure 22. The relative displacement of superstructure against substructure histories under Kobe (Japan) earthquake.

Figure 23 shows that the maximum force that pier one experience under Kobe (Japan) earthquake is 12,669 N in case of only LRBPs. It is reduced to 8707 N with the implementation of the proposed system.

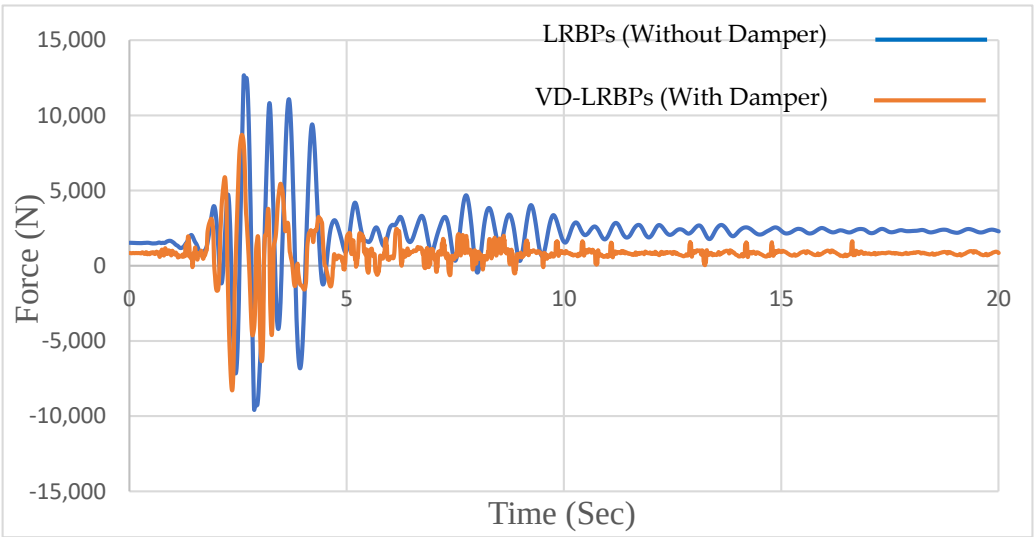

Figure 23. Force histories that pier 1 experiences under the Kobe (Japan) earthquake.

5.3. El Centro Ground Motion Record

The maximum displacement of superstructure against substructure (bearings displacement) under the Imperial Valley (El Centro) earthquake for the case of only LRBPs is 38 mm. However, using VD-LRBPs reduced this amount to 14 mm (Figure 24).

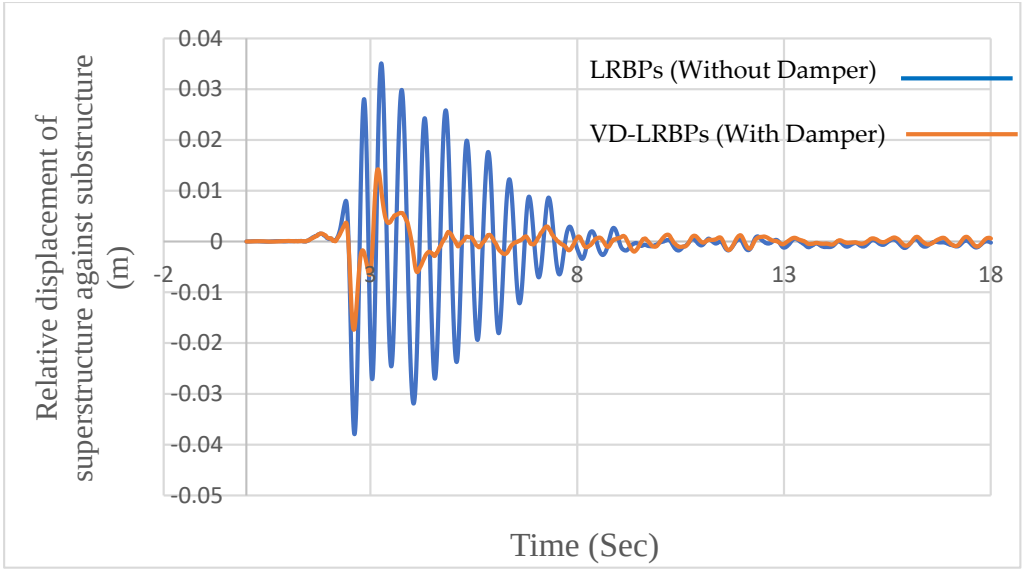

Figure 24. The relative displacement of superstructure against substructure histories under Imperial Valley (El Centro) earthquake.

The maximum force pier one experienced under the El Centro ground motion in the case of implementing only LRBPs is 12,556 N, while, in the case of using the VD-LRBPs system, it is reduced to 10,230 N (Figure 25).

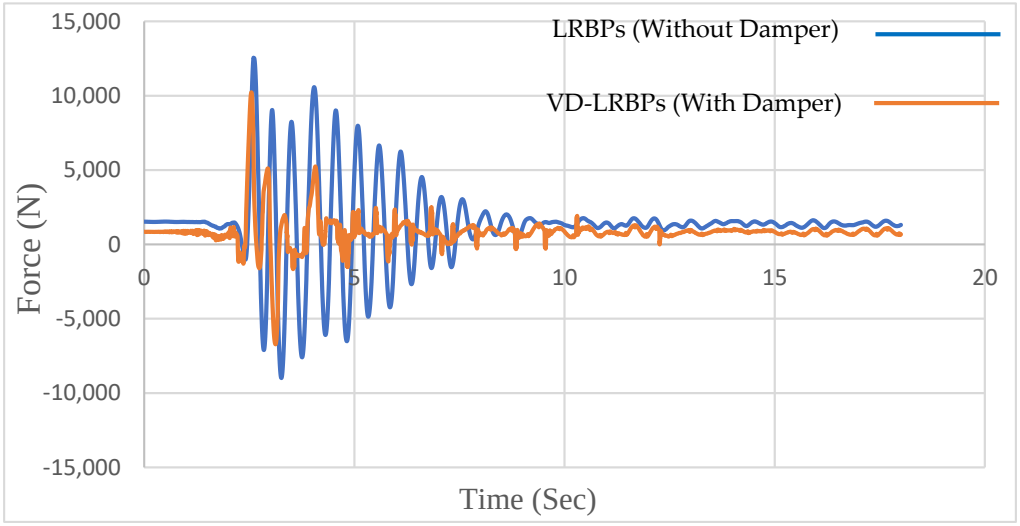

Figure 25. Force histories that pier one experiences under the Imperial Valley (El Centro) earthquake.

In summary, the beneficial effect of the system in reducing the relative displacement of superstructure with reference to the substructure is evident in all cases. This addresses the main objective of this investigation, which is limiting or eliminating the lateral sliding at the bearings, as well as the repeatability of the results for a variety of ground motion records. It has been observed that the most noticeable and drastic collapses have been associated with the transverse direction. The investigation of failures for small to medium span highway bridges with LRBPs has shown that among these damages, the failure of the shear key, joints and abutment failure, and span collapse are more prevalent. Therefore, limiting lateral movement will help reducing these damages. Nevertheless, such change of structural behavior may potentially and negatively affect other structural members. An example would be an increase in lateral forces to the substructures. However, forces transmitted to the piers do not necessarily follow a certain trend for all cases. For instance,

in the case of Northridge earthquake, the level of force is increased with the addition of VD, but the force is reduced for the case of other earthquakes. This increase can be attributed to the stiffening effect of the damper, and the reduction can be associated with the performance of the system in damping the energy and vibration with optimal design of VD for the specific case of other earthquakes.

6. Summary and Conclusions

One of the most common damages for the small to medium span steel and concrete highway bridges during a seismic event is the sliding between laminated rubber bearing pads (LRBP) and girders, also called sliding at bearing. This can cause expansion joint failure or even span collapse. Although investigations show that sliding at bearing can act as seismic isolation for the piers and limit the impact on substructure during intense earthquakes, the large displacement between superstructure and substructure in each span can cause span failure. Accordingly, proper restrainers need to be implemented to control the large displacement caused by the sliding at bearings. Among all types of restrainers, energy dissipation devices including viscous dampers have shown great capacity in absorbing earthquake energy and limiting the displacement. This study investigated the effectiveness of VD-LRBPs (Viscous Dampers combined with Bearing Pads) for controlling the large displacement between superstructure and substructure under several earthquakes in transverse direction. Accordingly, a finite element model validated with available experimental results in this study was used to conduct 3D nonlinear time history analysis (NTHA) of an RC bridge subjected to various ground motion records. The Northridge earthquake was implemented for initial investigation and fine tuning of the viscous damper for optimal performance. Subsequently, three other ground motion records, the TABAS (Iran) earthquake, the Kobe (Japan) earthquake, and the Imperial Valley were used to show reproducibility of the results and repeatability of the improving effects of the new system in the behavior of the bridge. It should be noted that the approach used in this study can be utilized for further refinement to produce better results for any specific ground motion and bridge structure. For all the analyses, the relative displacement of the superstructure with reference to the substructure and the force in the piers were recorded for two cases, with only LRBPs and with VD-LRBPs. The results show that the viscous damper effectively controls the relative displacement and helps self-centering of the superstructure by reducing the potential residual displacement to near zero. In addition, monitoring the force in the piers reveals that adding viscous damper, in most cases, also reduces the force transferred from superstructure to the substructure. Note that the potential exists for the inertia force transmitted from the superstructure to the piers in some cases. This increase was shown to be relatively small and no cause for concern compared to highly beneficial contribution of the damper in dissipating earthquake energy and reducing displacements. It is expected that the results of this study pave the way for application of the system in seismic zones.

Author Contributions: Conceptualization, S.S.K.D. (Seyed Saman Khedmatgozar Dolati), S.S.K.D. (Seyed Sasan Khedmatgozar Dolati) and A.M.; methodology, S.S.K.D. (Seyed Saman Khedmatgozar Dolati), S.S.K.D. (Seyed Sasan Khedmatgozar Dolati) and A.M.; software, S.S.K.D. (Seyed Saman Khedmatgozar Dolati) and S.S.K.D. (Seyed Sasan Khedmatgozar Dolati); validation, S.S.K.D. (Seyed Saman Khedmatgozar Dolati). and A.M.; formal analysis, S.S.K.D. (Seyed Saman Khedmatgozar Dolati) and S.S.K.D. (Seyed Sasan Khedmatgozar Dolati); investigation, S.S.K.D. (Seyed Saman Khedmatgozar Dolati), S.S.K.D. (Seyed Sasan Khedmatgozar Dolati) and A.M.; resources, S.S.K.D. (Seyed Saman Khedmatgozar Dolati), S.S.K.D. (Seyed Sasan Khedmatgozar Dolati) and A.M.; data curation, S.S.K.D. (Seyed Saman Khedmatgozar Dolati) and S.S.K.D. (Seyed Sasan Khedmatgozar Dolati); writing—original draft preparation, S.S.K.D. (Seyed Saman Khedmatgozar Dolati); writing—review and editing, A.M.; visualization, S.S.K.D. (Seyed Saman Khedmatgozar Dolati), S.S.K.D. (Seyed Sasan Khedmatgozar Dolati) and A.M.; supervision, A.M. All authors have read and agreed to the published version of the manuscript.

Funding: This research received no external funding.

Data Availability Statement: The data presented in this study are available on request from the corresponding author.

Acknowledgments: The authors greatly acknowledge the internal support by the Department of Civil and Environmental Engineering at Florida International University. The contents of this paper reflect the views of the authors, who are responsible for the facts and the accuracy of the information presented herein.

Conflicts of Interest: The authors declare that they have no known competing financial interests or personal relationships that could have appeared to influence the work reported in this paper.

References

1. Kawashima, K.; Takahashi, Y.; Ge, H.; Wu, Z.; Zhang, J. Reconnaissance report on damage of bridges in 2008 Wenchuan, China, earthquake. *J. Earthq. Eng.* **2009**, *13*, 965–996. [CrossRef]
2. Xiang, N.; Goto, Y.; Obata, M.; Alam, M.S. Passive seismic unseating prevention strategies implemented in highway bridges: A state-of-the-art review. *Eng. Struct.* **2019**, *194*, 77–93. [CrossRef]
3. Kawashima, K.; Unjoh, S.; Hoshikuma, J.-I.; Kosa, K. Damage of bridges due to the 2010 Maule, Chile, earthquake. *J. Earthq. Eng.* **2011**, *15*, 1036–1068. [CrossRef]
4. Schanack, F.; Valdebenito, G.; Alvial, J. Seismic damage to bridges during the 27 February 2010 magnitude 8.8 Chile earthquake. *Earthq. Spectra* **2012**, *28*, 301–315. [CrossRef]
5. Buckle, I. *The Northridge, California Earthquake of January 11, 1994: Performance of Highway Bridges*; Tech. Rep; NCEER: New York, NY, USA, 1994.
6. Xiang, N.; Li, J. Seismic Performance of Highway Bridges with Different Transverse Unseating-Prevention Devices. *J. Bridg. Eng.* **2016**, *21*, 4016045. [CrossRef]
7. Li, J.; Xiang, N.; Tang, H.; Guan, Z. Shake-table tests and numerical simulation of an innovative isolation system for highway bridges. *Soil Dyn. Earthq. Eng.* **2016**, *86*, 55–70. [CrossRef]
8. Xiang, N.; Li, J. Experimental and numerical study on seismic sliding mechanism of laminated-rubber bearings. *Eng. Struct.* **2017**, *141*, 159–174. [CrossRef]
9. Maghsoudi-Barmi, A.; Khaloo, A. Experimental investigation of life-time performance of unbounded natural rubber bearings as an isolation system in bridges. *Struct. Infrastruct. Eng.* **2021**, *17*, 1096–1109. [CrossRef]
10. Xiang, N.; Goto, Y.; Alam, M.S.; Li, J. Effect of bonding or unbonding on seismic behavior of bridge elastomeric bearings: Lessons learned from past earthquakes in China and Japan and inspirations for future design. *Adv. Bridg. Eng.* **2021**, *2*, 14. [CrossRef]
11. Zhang, B.; Wang, K.; Lu, G.; Guo, W. Seismic Response Analysis and Evaluation of Laminated Rubber Bearing Supported Bridge Based on the Artificial Neural Network. *Shock Vib.* **2021**, *2021*, 5566874.
12. Han, Q.; Du, X.; Liu, J.; Li, Z.; Li, L.; Zhao, J. Seismic damage of highway bridges during the 2008 Wenchuan earthquake. *Earthq. Eng. Eng. Vib.* **2009**, *8*, 263–273. [CrossRef]
13. Li, J.; Peng, T.; Xu, Y. Damage investigation of girder bridges under the Wenchuan earthquake and corresponding seismic design recommendations. *Earthq. Eng. Eng. Vib.* **2008**, *7*, 337–344. [CrossRef]
14. Chang, K.C.; Kuo, K.Y.; Liu, K.Y.; Lu, C.H. On seismic retrofit strategies of highway bridges-experiences learned from Chi-Chi earthquake. In Proceedings of the 13th World Conference on Earthquake Engineering, Vancouver, BC, Canada, 1–6 August 2004.
15. Lu, C.-H.; Liu, K.-Y.; Chang, K.-C. Seismic performance of bridges with rubber bearings: Lessons learnt from the 1999 Chi-Chi Taiwan earthquake. *J. Chin. Inst. Eng.* **2011**, *34*, 889–904. [CrossRef]
16. Kuang-Yen, L.; Kuo-Chun, C. Parametric study on performance of bridge retrofitted by unseating prevention devices. *Earthq. Eng. Eng. Vib.* **2006**, *5*, 111–118. [CrossRef]
17. Filipov, E.T.; Revell, J.R.; Fahnestock, L.A.; LaFave, J.M.; Hajjar, J.F.; Foutch, D.A.; Steelman, J.S. Seismic performance of highway bridges with fusing bearing components for quasi-isolation. *Earthq. Eng. Struct. Dyn.* **2013**, *42*, 1375–1394. [CrossRef]
18. Filipov, E.T.; Fahnestock, L.A.; Steelman, J.S.; Hajjar, J.F.; LaFave, J.M.; Foutch, D.A. Evaluation of quasi-isolated seismic bridge behavior using nonlinear bearing models. *Eng. Struct.* **2013**, *49*, 168–181. [CrossRef]
19. Steelman, J.S. *Sacrificial Bearing Components for Quasi-Isolated Response of Bridges Subject to High-Magnitude, Low-Probability Seismic Hazard*; University of Illinois at Urbana-Champaign: Champaign, IL, USA, 2013; ISBN 1303803127.
20. Moslehi Tabar, A.; De Domenico, D.; Dindari, H. Seismic Rehabilitation of Steel Arch Bridges Using Nonlinear Viscous Dampers: Application to a Case Study. *Pract. Period. Struct. Des. Constr.* **2021**, *26*, 4021012. [CrossRef]
21. Mavrakis, G. Greece's new high-speed railway line: Detailed design and construction engineering of bridge SG26. *Ce/Papers* **2021**, *4*, 249–254. [CrossRef]
22. Liu, Q.; Zhu, S.; Yu, W.; Wu, X.; Song, F.; Ren, X. Ground Motion Frequency Insensitivity of Bearing-Supported Pedestrian Bridge with Viscous Dampers. *KSCE J. Civ. Eng.* **2021**, *25*, 2662–2673. [CrossRef]
23. Hu, X.; Zhang, R.; Ren, X.; Pan, C.; Zhang, X.; Li, H. Simplified design method for structure with viscous damper based on the specified damping distribution pattern. *J. Earthq. Eng.* **2020**, *2020*, 1–21. [CrossRef]
24. Zhou, L.; Wang, X.; Ye, A. Shake table test on transverse steel damper seismic system for long span cable-stayed bridges. *Eng. Struct.* **2019**, *179*, 106–119. [CrossRef]

25. Xu, Y.; Wang, R.; Li, J. Experimental verification of a cable-stayed bridge model using passive energy dissipation devices. *J. Bridg. Eng.* **2016**, *21*, 4016092. [CrossRef]
26. Dai Nguyen, X.; Guizani, L. Analytical and numerical investigation of natural rubber bearings incorporating U-shaped dampers behaviour for seismic isolation. *Eng. Struct.* **2021**, *243*, 112647. [CrossRef]
27. Tang, H.; Li, J.Z. Displacement control method for continuous bridges on laminated rubber bearings under earthquake excitation. *China J. Highw. Transp.* **2013**, *26*, 110–116.
28. Jiang, J.; Li, J.; Fan, L. Study on Aseismic Performance of Combination of Laminated Rubber Bearing and Viscous Damper for Bridge. *J. Highw. Transp. Res. Dev.* **2005**, *2005*, 8.
29. Xiang, N.; Alam, M.S.; Li, J. Yielding steel dampers as restraining devices to control seismic sliding of laminated rubber bearings for highway bridges: Analytical and experimental study. *J. Bridg. Eng.* **2019**, *24*, 4019103. [CrossRef]
30. AASHTO. *AASHTO LRFD Bridge Design Specifications*, 8th ed.; American Association of State Highway and Transportation Officials: Washington, DC, USA, 2017.
31. Laminated Rubber Bearing Pad. Available online: https://civildigital.com/base-isolation-system-outline-on-principles-types-advantages-applications/ (accessed on 1 October 2021).
32. Ghiasian, M.; Fakher, A.; Khanmohammadi, M. Enhancing the Seismic Performance of Batter Piles in Pile-Supported Wharves Using Fluid Viscous Dampers. Available online: https://www.researchgate.net/profile/Mohammad-Ghiasian/publication/344978757_Enhancing_the_seismic_performance_of_batter_piles_in_pile-supported_wharves_using_fluid_viscous_dampers/links/5fa1ec04458515b7cfba41a6/Enhancing-the-seismic-performance-of-batter-piles-in-pile-supported-wharves-using-fluid-viscous-dampers.pdf (accessed on 1 October 2021).
33. Soneji, B.B.; Jangid, R.S. Passive hybrid systems for earthquake protection of cable-stayed bridge. *Eng. Struct.* **2007**, *29*, 57–70. [CrossRef]
34. Martínez-Rodrigo, M.D.; Filiatrault, A. A case study on the application of passive control and seismic isolation techniques to cable-stayed bridges: A comparative investigation through non-linear dynamic analyses. *Eng. Struct.* **2015**, *99*, 232–252. [CrossRef]
35. Xu, Y.; Tong, C.; Li, J. Simplified calculation method for supplemental viscous dampers of cable-stayed bridges under near-fault ground motions. *J. Earthq. Eng.* **2021**, *25*, 65–81. [CrossRef]
36. Tabatabai, H.; Mehrabi, A.B. Design of mechanical viscous dampers for stay cables. *J. Bridg. Eng.* **2000**, *5*, 114–123. [CrossRef]
37. Zhu, J.; Zhang, W.; Zheng, K.F.; Li, H.G. Seismic design of a long-span cable-stayed bridge with fluid viscous dampers. *Pract. Periodical Struct. Des. Constr.* **2016**, *21*, 04015006. [CrossRef]
38. Li, J.; Yan, J.; Peng, T.; Han, L. Shake table studies of seismic structural systems of a Taizhou Changjiang highway bridge model. *J. Bridg. Eng.* **2015**, *20*, 4014065. [CrossRef]
39. Guo, T.; Liu, J.; Huang, L. Investigation and control of excessive cumulative girder movements of long-span steel suspension bridges. *Eng. Struct.* **2016**, *125*, 217–226. [CrossRef]
40. Kiran, J.; Krishnakumar, S.; Alex, F.; Mohanan, N. Seismic Performance of a Pre stressed Tied Arch bridge Fitted With Dampers. *Int. Res. J. Eng. Technol.* **2016**, *3*, 1454–1460.
41. Agrawal, A.K.; Amjadian, M. Seismic component devices. In *Innovative Bridge Design Handbook*; Elsevier: Amsterdam, The Netherlands, 2016; pp. 531–553.
42. Lee, D.; Taylor, D.P. Viscous damper development and future trends. *Struct. Des. Tall Build.* **2001**, *10*, 311–320. [CrossRef]
43. Xiang, N.; Alam, M.S.; Li, J. Shake table studies of a highway bridge model by allowing the sliding of laminated-rubber bearings with and without restraining devices. *Eng. Struct.* **2018**, *171*, 583–601. [CrossRef]
44. Yi, J.; Zhou, J.; Ye, X. Seismic Control of Cable-stayed Bridge Using Negative Stiffness Device and Fluid Viscous Damper under Near-field Ground Motions. *J. Earthq. Eng.* **2020**, *2020*, 1–18. [CrossRef]
45. Wen, J.; Han, Q.; Xie, Y.; Du, X.; Zhang, J. Performance-based seismic design and optimization of damper devices for cable-stayed bridge. *Eng. Struct.* **2021**, *237*, 112043. [CrossRef]